PROCEEDINGS OF SPIE

SPIEDigitalLibrary.org/conference-proceedings-of-spie

Carrier dynamics in TMDCs for optical applications

J. Hader, J. V. Moloney, L. Meckbach, T. Stroucken, S. W. Koch

J. Hader, J. V. Moloney, L. Meckbach, T. Stroucken, S. W. Koch, "Carrier dynamics in TMDCs for optical applications," Proc. SPIE 10920, 2D Photonic Materials and Devices II, 109200I (27 February 2019); doi: 10.1117/12.2510682

SPIE.

Event: SPIE OPTO, 2019, San Francisco, California, United States

Carrier dynamics in TMDCs for optical applications

J. Hader[a], J.V. Moloney[a], L. Meckbach[b], T. Stroucken[b], and S.W. Koch[b].

[a]College of Optical Sciences, The University of Arizona,
1630 East University Boulevard, Tucson, Arizona 85721, USA;

[d]Department of Physics and Material Sciences Center, Philipps-Universit{i}at Marburg,
Renthof 5, 35032 Marburg, Germany;

ABSTRACT

Fully microscopic many-body models based on the Dirac-Bloch equations and quantum-Boltzmann type scattering equations are used to study the carrier dynamics in monolayer transition metal dichalcogenides (TMDCs) under conditions as typical for applications as lasers, diodes or saturable absorbers. The carrier-carrier scattering is shown to be happening on an ultra-fast few-femtosecond timescale for excitations high above the bandgap. Once the carriers have relaxed into quasi-equilibrium distributions near the bandgap, the scattering is slowed dramatically by phase-space filling and screening of the Coulomb interaction. Here, the scatterings and resulting dephasing of the optical polarizations happen on a 100fs timescale and lead to similar broadenings as found in conventional III-V semiconductor materials. Also like the case in III-V materials, the carrier phonon scattering times are found to be in the picosecond range. The scatterings are shown to allow for gain spectra as needed for good lasing operation. It is shown that the weak interaction between the two bands associated with the two different sub-lattices can potentially allow for simultaneous lasing at two different frequencies. Strong absorption and ultrafast carrier relaxation could allow for TMDCs to be used in saturable absorption applications.

Keywords: TMDC, many-body theory, Dirac Bloch equations, carrier scattering, absorption, gain

1. INTRODUCTION

Single layer transition-metal dichalcogenide crystals (TMDCs) have been found to exhibit remarkable electronic and optical properties which make them interesting for various technical applications.[1–4] Unlike their bulk counterparts, many single layer TMDCs have a direct bandgap as required for efficient optical absorbers or emitters and, for many of them, the bandgap lies in the technically important wavelength range spanning from the near infrared to the visible. Meanwhile they exhibit characteristics that significantly differ from more conventional III-V or II-VI semiconductor materials. The direct bandedge is not at the single zero momentum Gamma point but at the six non-zero momentum K-points of the Brillouin zone. The lack of inversion symmetry together with strong relativistic spin-orbit coupling lead to a bandstructure that allows for controlled excitation into different bandstructure minima (valleys) using selective light polarizations. The spin-valley coupling suppresses spin and valley relaxation and allows for TMDCs to be used for valleytronics and spintronics.[5,6]

Also, the Coulomb interaction has been shown to be dramatically stronger than in the more conventional materials with exciton binding energies in the hundreds of meV rather than only a few meV.[4] The excitonic resonances have been found to dominate optical spectra at low excitation even at room temperature where they are mostly invisible in the more conventional semiconductor materials. The Coulomb interaction also leads to a strong enhancement of the absorption which makes the material interesting for absorber applications.

The strong Coulomb interaction together with the peculiarities of the bandstructure require significant changes of the theory used to describe the microscopic many-body physics in TMDCs as compared to the case in more conventional materials. While the semiconductor Bloch equations have been used with great success to describe the optical and electronic interactions in conventional materials, it has been shown that these equations have to be extended to the so-called Dirac-Bloch equations for the description of TMDCs.[7,8] Here, the single particle states are described by two-component spinors rather than single component wavefunctions in order to

J. H.: Electronic mail: jhader@acms.arizona.edu

2D Photonic Materials and Devices II, edited by Arka Majumdar, Carlos M. Torres, Hui Deng, Proc. of SPIE Vol. 10920, 109200I · © 2019 SPIE · CCC code: 0277-786X/19/$18 · doi: 10.1117/12.2510682

be able to account for different spin and valley components. Moreover, the strong Coulomb interaction prohibits the a priori neglect of processes which have been found negligible in conventional materials. E.g., Auger-like processes appear in the Coulomb-induced renormalization of energies and the matter-field coupling. In turn, this leads to a non-trivial coupling between microscopic optical polarizations and occupation probabilities which leads to the fact that the ground-state in the absence of optical excitation is no longer given by the case of zero occupations and polarizations.

The Dirac-Bloch equations were used successfully in the past to calculate absorption and gain spectra for single and multiple layers of TMDCs.[8,9] Here, we extend the model as used there to also include incoherent interactions due to electron-electron and electron-phonon scattering in order to study carrier dynamics and to determine self-consistently the dephasing of the optical polarizations and resulting broadening of optical spectra. Ref.[9] found optical gain in monolayer TMDCs which should allow for successful lasing applications. However, there, the dephasing of the polarizations was modeled using a simple dephasing time approach with a broadening parameter as typical for conventional semiconductor materials. As will be shown here, the strong Coulomb interaction can lead to much faster carrier-carrier scattering dynamics in TMDC then in the conventional materials. This could lead to extremely strong spectral broadening which would diminish the gain amplitudes. Here we use the extended model to calculate a priori the scattering induced spectral broadening. The model is also used to study the purely incoherent carrier dynamics after optical or electronic excitations in order to test the applicability of TMDCs for applications like saturable absorbers.

2. THEORETICAL BACKGROUND

The theoretical approach as used here is based on the Dirac Bloch equations as described in Refs.[8,9] and Refs. therein. These are the equations of motions for microscopic polarizations, $p_{\mathbf{k}s\tau}$, and occupation probabilities for electrons/holes, $f^{e/h}_{\mathbf{k}s\tau}$:

$$\begin{aligned} i\hbar\frac{d}{dt}p_{\mathbf{k}s\tau} &= \left(\varepsilon^{e}_{\mathbf{k}s\tau}-\varepsilon^{h}_{\mathbf{k}s\tau}\right)p_{\mathbf{k}s\tau}-\left(1-f^{e}_{\mathbf{k}s\tau}-f^{h}_{\mathbf{k}s\tau}\right)\Omega_{\mathbf{k}s\tau}-i\hbar\left.\frac{d}{dt}p_{\mathbf{k}s\tau}\right|_{\text{corr}}, \\ \frac{d}{dt}f^{e/h}_{\mathbf{k}s\tau} &= -\frac{2}{\hbar}\,\text{Im}\left(\Omega_{\mathbf{k}s\tau}p^{*}_{\mathbf{k}s\tau}\right)-\left.\frac{d}{dt}f^{e/h}_{\mathbf{k}s\tau}\right|_{\text{corr}}. \end{aligned} \tag{1}$$

Here, $\mathbf{k}$ is the in-plane momentum and s and τ are the spin- and valley-indices. While these equations take the same form as the conventional semiconductor Bloch equations (SBE), significant differences are hidden within the renormalized single-particle energies ε and the renormalized field (effective Rabi frequency), Ω. E.g., the energy renormalizations contain a contribution involving the polarizations which would be absent in the semiconductor Bloch equations:

$$\begin{aligned} \varepsilon^{e/h}_{\mathbf{k}s\tau} = \epsilon^{e/h}_{\mathbf{k}s\tau} &- \sum_{\mathbf{k}'}V_{|\mathbf{k}-\mathbf{k}'|}\left[W^{s\tau}_{cccc/vvvv}\left(\mathbf{k},\mathbf{k}'\right)-W^{s\tau}_{cvvc/vccv}\left(\mathbf{k},\mathbf{k}'\right)\right]f^{e/h}_{\mathbf{k}'s\tau}+ \\ &\sum_{\mathbf{k}'}V_{|\mathbf{k}-\mathbf{k}'|}\left[W^{s\tau}_{ccvc/vcvv}\left(\mathbf{k},\mathbf{k}'\right)p_{\mathbf{k}'s\tau}+c.c\right]. \end{aligned} \tag{2}$$

Similar terms involving the occupations are contained within the renormalized field. These terms lead to a non-trivial ground-state for the system.

In the renormalizations, V is the bare 2D Coulomb potential and W are overlaps between electron (c) and hole (v) wavefunctions.[8] Coulomb matrix elements including $W_{ccvc/vcvv}$ describe Auger-like processes which in the case of conventional materials are many orders of magnitude smaller than the direct terms in the first line of Eq.(2).

ϵ are the single particle energies. As in Refs.,[8,9] we use an effective four-band model. This includes the so-called A and B bands which are the lowest two electron and highest two hole bands at the K-points which are non-degenerate due to the spin-orbit splitting.[5] Bandstructure parameters are determined by fitting to the results of first principle DFT calculations.

The last terms in Eq.(1) describe higher order correlations beyond the Hartree-Fock limit. These describe electron-electron and electron-phonon scatterings as well as the screening of the Coulomb interaction. Here, we explicitly include the scattering processes within the second-Born and Markov-approximations. On this level, they take the form of quantum-Boltzmann scattering equations. Like the Dirac-Bloch equations, the scattering equations for TMDCs contain contributions that are absent in the corresponding equations for conventional materials. We tested that for typical device applications with non-cryogenic temperatures and average excitation densities these terms are negligible for the TMDCs. Thus, the scattering equations take the same form as shown for III-V materials in Ref.[10]

Photoluminescence (PL) spectra are calculated by solving the equations of motions for photon-assisted polarizations. These equations are the so-called semiconductor luminescence equations (SLE).[11,12] Neglecting, as for the scatterings, terms that are absent for typical III-V materials, the SLE take the same form as the SBE, except that the inversion factor $\left(1 - f^e_{\mathbf{k}s\tau} - f^h_{\mathbf{k}s\tau}\right)$ is replaced by $\left(f^e_{\mathbf{k}s\tau} f^h_{\mathbf{k}s\tau}\right)$ and an additional source term which is due to higher excitonic correlations. The latter is numerically expensive to calculate. However, it significantly influences the PL amplitude and the resulting radiative carrier lifetime, especially in systems where, as here, the Coulomb interaction is very strong.[13] Also, neglecting these contributions leads in general to spectra that contain non-physical negative PL. As for the optical polarization, we calculate the dephasing of the photon assisted polarization due to carrier scatterings explicitly.

3. RESULTS

3.1 Carrier dynamics

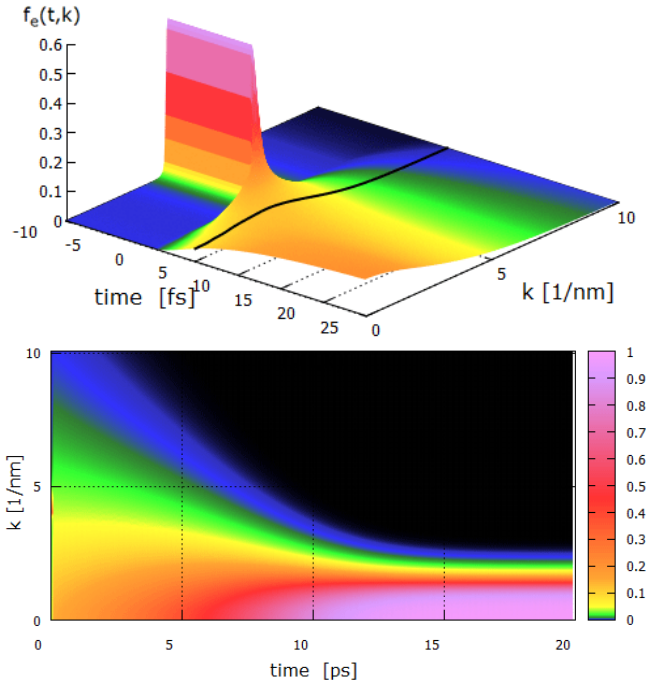

Figure 1: Time- and momentum-resolved occupation probability for electrons in the A conduction band for a monolayer of $MoTe_2$ suspended in air at 300 K. The occupations were initialized before the relaxations were turned on using a 50 fs Gaussian pulse centered at 1.4 eV with an amplitude of 10^8 V/m.Carrier relaxations due to scatterings were turned on at t=0 s. Top/bottom: fast initial/slow long term dynamics. The black line in the upper picture shows is a contour of the distribution 5 fs after the relaxation was turned on.

Fig.1 shows the carrier dynamics due to electron-electron and electron-phonon scattering in a monolayer of $MoTe_2$ that is suspended in air and at 300 K. For this example only the top electron and hole A-bands were

taken into account. The system was initialized by creating a carrier distribution using a 50 fs Gaussian optical pulse with an amplitude of 10^8 V/m. The pulse has a center energy of 1.4 eV and creates carriers about 200 meV above the free carrier electron and hole bandedges. Carrier dynamics due to the scatterings are turned off during the creation of these initial distributions in order to allow to see the effect of the relaxation separate from the pump dynamics. After the optical pulse is gone, the scatterings are turned on.

As can be seen in Fig. 1, the carrier distributions relax toward the bandgap on a few femtosecond timescale. This fast dynamic is due to the strong Coulomb interaction. For comparison, in typical III-V materials this relaxation would take place on a timescale of several tens of fs to few hundreds of fs. After about 10 fs, the carriers are already relaxed into a quasi equilibrium Fermi distribution. However, this is a very hot distribution at initially about 7000 K. The electron-phonon scattering then cools this distribution down to the assumed lattice temperature of 300 K. The latter scatterings take place on a timescale of several picoseconds which is of the same order as in the case of III-V semiconductors.

3.2 Optical spectra

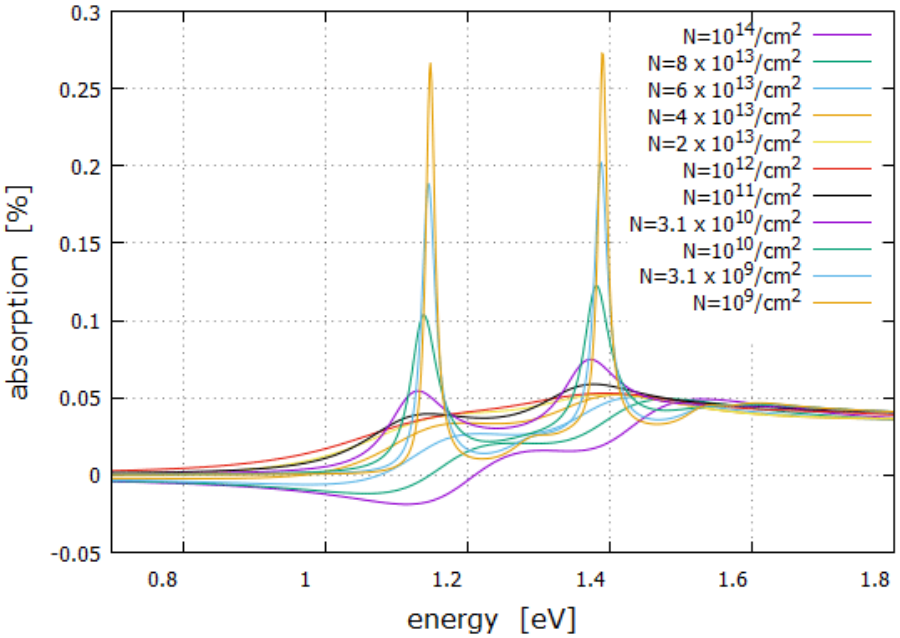

Figure 2: Absorption for a monolayer of $MoTe_2$ suspended in air at 300 K and for various carrier densities. The carrier densities in the label are the ones for the A-bands and the same density is assumed to be also in the B-bands.

The ultra-fast carrier dynamics as seen in Sec.3.1 could also have severe consequences on optical spectra. If the carrier-polarization scattering is on the same, few fs-timescale as the initial carrier relaxation seen in the example above, it would lead to line-broadenings on the order of several hundreds of meV to one eV. This would mean that e.g. gain spectra would be extremely broadened and, thus, made shallow. In turn, this would make it very hard to achieve sufficient gain to overcome the losses involved in laser operations.

To test the effects of the electron and electron-phonon scatterings on the optical spectra in TMDC we calculated absorption and PL spectra for the example of a mono-layer $MoTe_2$ that is suspended in air and at 300 K. Fig.2 shows the absorption for various carrier densities. We assume that the density in the A- and B-bands is the same. This should be a fair approximation assuming optical excitation above the B-bandedge since both bands have similar absorption strength in that spectral region.

With increasing carrier density and corresponding carrier-carrier scattering the linewidth of the excitonic resonances increases. At the same time, the increasing densities lead to an increased screening of the Coulomb

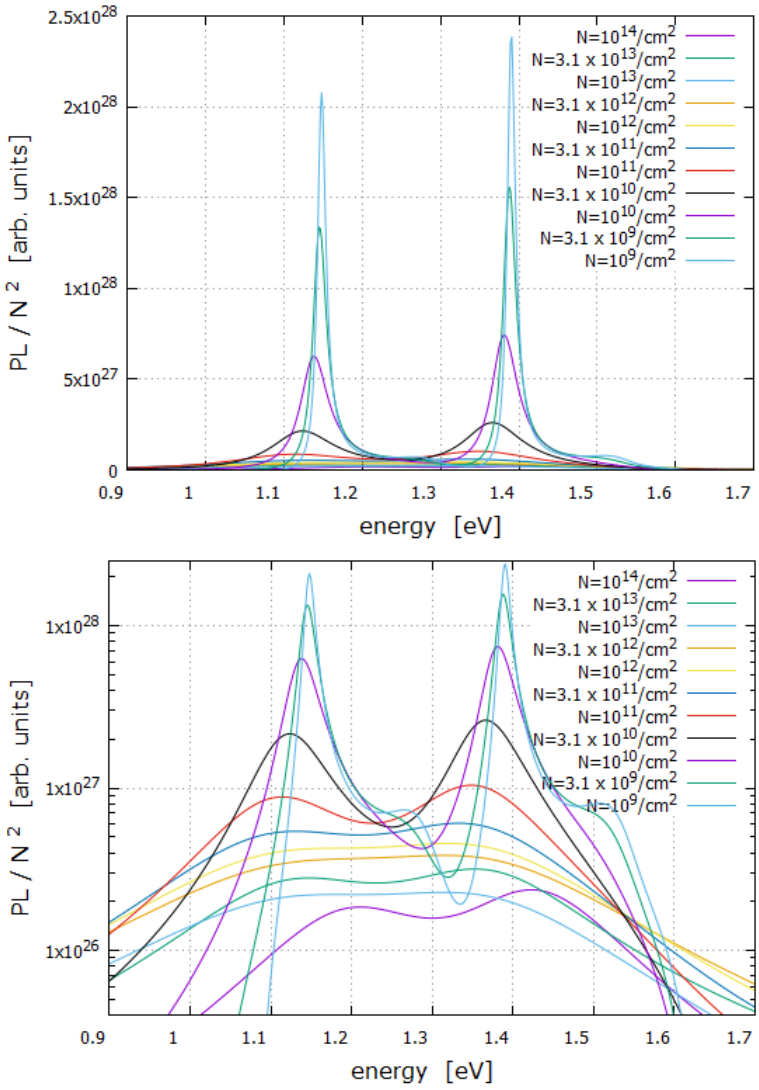

Figure 3: PL for a monolayer of $MoTe_2$ suspended in air at 300 K and for various carrier densities. Top/bottom: linear, logarithmic scale.

interaction and increased bandgap renormalizations. The former reduces the exciton binding energy and oscillator strength. The latter leads to a red-shift of the bandgap. In the low density regime, these effects lead to a red-shift of the absorption edge. At very high densities the gain maximum shifts blue with increasing density. This is caused by phase space filling.

The linewidths as seen in Fig.3 are smaller than what one might expect from the relaxation rates as seen in Fig.1 and fairly comparable to those typical for III-V semiconductors. The reason for the rather moderate broadenings is that for carriers in thermal equilibrium distributions near the bandgap the screening is far more effective than if the same amount of carriers would be located energetically above the gap as initially in Sec.3.1. Also, the carrier scatterings are reduced for the distributions here since the final states for scattering transitions are already occupied to a high degree and, thus, do not allow for further in-scattering.

As mentioned in the introduction, the A and B bands do not couple due to spin and valley selection rules. Thus, carriers excited into the B-band do not relax to the energetically lower A-band on the timescales as relevant for the processes investigated here. This allows for a build up of inversion in the B band high above

the fundamental bandedge. While not occurring for the parameters studied here, this could open the possibility of two simultaneous gain maxima which could allow for unusually wide lasing tuning ranges, two color lasing or interesting spin-selective lasing at different frequencies.

The fact that the A and B band do not couple and allow for significant carrier densities in both bands at the same time also allows for significant spontaneous emission from both bands. Fig. 3 shows PL spectra for this case. As in the absorption, the PL linewidth increases significantly with increasing density due to increasing scatterings and the spectra shift red with increasing density due to screening and energy renormalization. At densities in the density regime the spectra shift blue due to phase space filling. In the low density regime, where distributions can be approximated by Boltzmann distributions, the integrated PL scales with the density squared. As can be seen in Fig.3 where the spectra are scaled by the inverse of the square of the density, the scaling becomes significantly less than that at elevated densities. As has been shown in Ref.??, phase space filling at elevated densities significantly reduces the increase of the PL and, thus, the radiative carrier recombination rate.

4. SUMMARY

Fully microscopic many-body models are used to study the carrier dynamics in monolayer TMDCs. The theory is based on the Dirac-Bloch equations where incoherent processes due to electron-electron and electron-phonon scatterings are calculated explicitly by solving the corresponding quantum-Boltzmann type scattering equations. The model is used to study the carrier relaxation after an initial excitation above the bandgap in a layer of $MoTe_2$ suspended in air. It is shown that the strong Coulomb interaction in the TMDCs allows for ultrafast carrier scattering. A relaxation time due to electron-electron scattering of only a few femtoseconds is found for situations as they can arise in applications as in saturable absorbers. While this is more than an order faster than in typical III-V materials, the phonon scattering, which cools the carrier distributions down after the initial relaxation, is found to happen on a similar timescale as in the more conventional materials.

For situation as typical for light emission applications like lasers or LEDs where the carriers occupy quasi equilibrium distributions close to the bandgap, the scatterings are found to be rather similar to the conventional materials. Phase space filling and screening reduce the electron-electron scattering rates significantly in these situations.

The fact that the A and B bands do not couple due to spin and valley selection rules leads to independent Fermi levels for the two bands. Thus, inversion in the B band can occur at energies above the inversion range for the A band. This could allow for simultaneous emission from two separate spectral regions and could allow for technical applications where gain at different spectral regions is desired or gain regions with different spin and valley selection rules.

ACKNOWLEDGEMENTS

This material is based upon work supported by the Air Force Office of Scientific Research under award number FA9550-17-1-0246.

REFERENCES

1. K.F. Mak, C. Lee, J. Hone, J. Shan, and T.F. Heinz, "Atomically thin MoS_2: A new Direct-Gap Semiconductor," Phys. Rev. Lett. 105, 136805 (2010).
2. A. Splendiani, L. Sun, Y. Zhang, T. Li, J. Kim, C.Y. Chim, G. Galli, and F. Wang, "Emerging Photoluminescence in Monolayer MoS_2," Nano Lett., 2010, 10 (4), 1271-1275 (2010).
3. Q.H. Wang, K. Kalantar-Zadeh, A. Kis, J.N. Coleman, and M.S. Strano, "Electronics and optoelectronics of two-dimensional transition metal dichalcogenides," Nat. Nanotech. 7, 699-712 (2012).
4. F. Xia, H. Wang, D. Xiao, M. Dubey, and A. Ramasubramaniam, "Two-dimensional material nanophotonics," Nat. Photon. 8, 899-907 (2014).
5. D. Xiao, G.-B. Liu, W. Feng, X. Xu, and W. Yao, "Coupled Spin and Valley Physics in Monolayers of MoS_2 and Other Group-VI Dichalcogenides," Phys. Rev. Lett. 108, 196802 (2012).

6. G. Plechinger, P. Nagler, A. Arora, R. Schmidt, A. Chernikov, J. Lupton, R. Bratschitsch, C. Schuller, and T. Korn, "Valley Dynamics of Excitons in Monolayer Dichalcogenides," Phys. Stat. Sol. RRL 11(7), 1700131 (2017).
7. T. Stroucken, and S.W. Koch, "Optical Properties of Graphene," ed. R. Binder, World Scientific Publishing, Singapore, Chap. 2, 43-84 (2017).
8. L. Meckbach, T. Stroucken, and S.W. Koch, "Influence of the effective layer thickness on the ground-state and excitonic properties of transition-metal dichalcogenide systems," Phys. Rev. B 97, 035425 (2018).
9. L. Meckbach, T. Stroucken, and S.W. Koch, "Giant excitation induced bandgap renormalization in TMDC monolayers," Appl. Phys. Lett. 112, 061104 (2018).
10. J. Hader, S.W. Koch, and J.V. Moloney, "Microscopic theory of gain and spontaneous emission in GaInNAs laser material," Sol.-Stat. Electron. 47, 513-521 (2003).
11. M. Kira, F. Jahnke, S.W. Koch, J.D. Berger, D.V. Wick, T.R. Nelson, G. Khitrova, and H.M. Gibbs, H. "Quantum Theory of Nonlinear Semiconductor Microcavity Luminescence Explaining "Boser" Experiments". Phys. Rev. Lett. 79(25), 5170âĂŞ5173 (1997).
12. M. Kira, and S.W. Koch, "Semiconductor Quantum Optics," Cambridge University Press , Cambridge, UK (2012).
13. J. Hader, J.V. Moloney, and S.W. Koch, "Investigation of droop-causing mechanisms in GaN-based devices using fully microscopic many-body theory," Proc. SPIE 8625, Gallium Nitride Materials and Devices VIII, 86251M (2013).
14. J. Hader, J.V. Moloney, and S.W. Koch, "Supression of carrier recombination in semiconductor lasers by phase-space filling," Appl. Phys. Lett. 87, 201112 (2005).